The Astrophysical Journal, Vol. 148, April 1967

THE SIZE AND POSITION OF THE X-RAY SOURCE IN THE CRAB NEBULA

During a recent rocket flight, we observed the 1–6 keV X-radiation from the Crab Nebula with a modulation collimator of high resolution. We find the emission region to be centered on the Crab and of finite size. These results are in agreement with those of the lunar occultation experiment carried out by Bowyer, Byram, Chubb, and Friedman (1964). The present measurement improves upon the earlier work in that it provides size and position information along two nearly perpendicular directions rather than the one direction of the lunar transit. Also, since the measurements of Sco X-1 (Gursky, Giacconi, Gorenstein, Waters, Oda, Bradt, Garmire, and Sreekantan 1966*a*, *b*) and the Crab Nebula were made with the same instrument during a single flight, we were able to directly observe the qualitatively different appearance in X-rays of a starlike source (Sco X-1) and a source of finite angular size (Crab).

The Crab Nebula was first positively identified as a strong X-ray source by the above-mentioned occultation experiment. Thus the Crab is now known to be bright in a frequency range from 10^7 to 10^{19} c/s. In the radio and optical regions, the radiation is believed to be synchrotron emission because of the observed high degrees of polarization. Although it has been argued that the observed X-rays represent an extension of the synchrotron radiation to higher energies (Woltjer 1964; Shklovskii 1966), there is no conclusive evidence that eliminates other possibilities, notably thermal emission from a hot plasma. Arguments in support of this latter mechanism have recently been presented by Morrison and Sartori (1967). In any case, the gross dynamics of the Crab Nebula must be affected in a significant way by the X-ray emission since the total radiated power in X-rays is comparable to that at optical wavelengths and greatly exceeds that at radio wavelengths. Thus, comparison of the detailed angular structure in the X-ray, optical, and radio regions should contribute materially toward our understanding of the Crab Nebula.

The data reported here were obtained during a sounding rocket flight on March 8, 1966. Observations of the bright X-ray source in Scorpio, Sco X-1, during the same flight yielded both a 20″ upper limit to its angular size and its position to a precision of 4 sq. arc min (Gursky *et al.* 1966*a*, *b*) which, in turn, made possible an identification of its optical counterpart (Sandage, Osmer, Giacconi, Gorenstein, Gursky, Waters, Bradt, Garmire, Sreekantan, Oda, Osawa, and Jugaku 1966). Both the Crab and Scorpio observations were made with the same optical X-ray sensor system. It consisted of proportional counters with 50-μ Be windows and 30 mg/cm^2 of xenon, a camera, and two four-grid modulation collimators, each with multiple $40'' \times 10^\circ$ (FWHM) angular transmission zones, or "bands," separated one from another by about 5′. These angular dimensions differed for the two (one "long" and one "short") collimators by about 5 per cent to provide a vernier effect which in principle permits one to identify the angular transmission band corresponding to a given peak in the X-ray data. The 16 mm camera took successive 1-sec exposures and simultaneously viewed a $12^\circ \times 8\overset{\circ}{.}5$ star field and a portion of each collimator. The collimators were illuminated by a diffuse light source in such a way that the X-ray transmission bands were imaged directly onto the image of the star field. This allowed us to project lines of position corresponding to each data peak directly onto the celestial sphere. The entire detection system viewed the sky through the front end of the Aerobee 150 rocket.

The observations were made in the following way. The rocket was pointed toward the Crab Nebula for a period of about 40 sec during which the jitter in the attitude control system caused the rocket to scan the Nebula at rates of several arc minutes per second. Directly following this sequence, the rocket was rolled 60° about its long axis, and a 40-sec "postroll" period provided data which yielded lines of position on the celestial sphere which cross at 60° those obtained during the "preroll" period. During the preroll and postroll periods there were, respectively, nine and four transits of the optical Crab by the transmission bands of the short collimator. The long collimator made, respectively, nine and five transits during these periods.

The individual transits of the source did not appear as statistically significant peaks in the counting-rate data. Therefore, the optical aspect data, precise to 15″, were used to sum the data from the successive transits of the source region. For both the short and

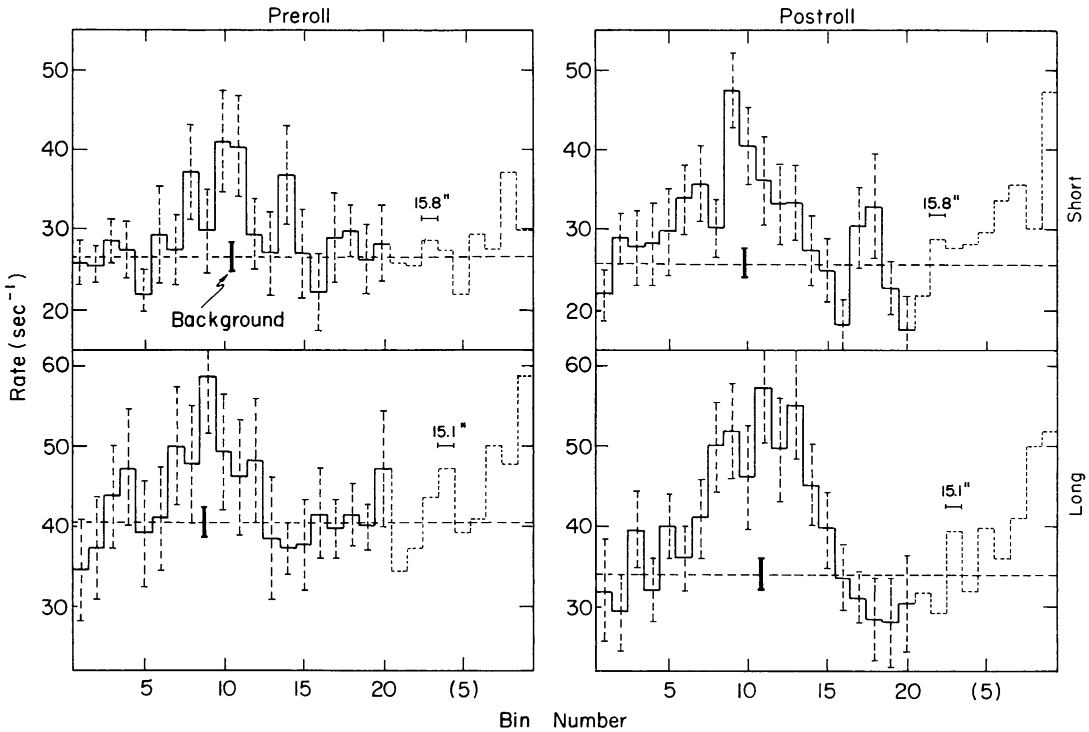

FIG. 1.—Data after initial superposition with periodicity equal to the angle of separation between adjacent transmission directions, namely, 5′1″.91 and 5′16″.62 for the long and short collimators, respectively. These angular intervals are divided into 20 equal bins and, in each histogram, the center of bin 10 represents the Becvar coordinates for the center of the Crab Nebula.

long collimators, the angular interval between two successive transmission bands was divided into 20 equal bins, each of approximately 15″ width. Both systems of 20 bins were fixed upon the celestial sphere, essentially superimposed, with bin 10 centered at (1950.0) $\alpha = 5^h31^m30^s$, $\delta = 21°59'$, the coordinates listed in the Becvar catalogue for the center of the Crab Nebula. In order to reduce the effects of background counts, we restricted the energy region studied to 1–6 keV. Each detected X-ray was credited to the bin which at that moment was being traversed by the center of a collimator transmission band. Also, the total time spent in each bin was accumulated. This superposition was carried out separately for each of the two collimators ("short" and "long") for both the preroll and postroll periods. The resultant rates with statistical errors are presented in Figure 1.

The centroid of the peak in each of the four sets of data in Figure 1 lies close to bin 10. Thus, in both scan directions, the center of the X-ray source lies close to the center of the

Crab. We further note that the occurrence of the "long" and "short" peaks at the same bin number eliminates from consideration most of the other celestial positions which, due to the multiplicity of transmission directions through the collimator, might be candidates for the location of the X-ray source. The background rates indicated in Figure 1 with their statistical errors were calculated from the rates in the 8 or 9 bins most removed from the peak. In each case they are consistent with the rates of about equivalent statistical significance obtained during the gross maneuvers of the rocket prior to and subsequent to the Crab observations.

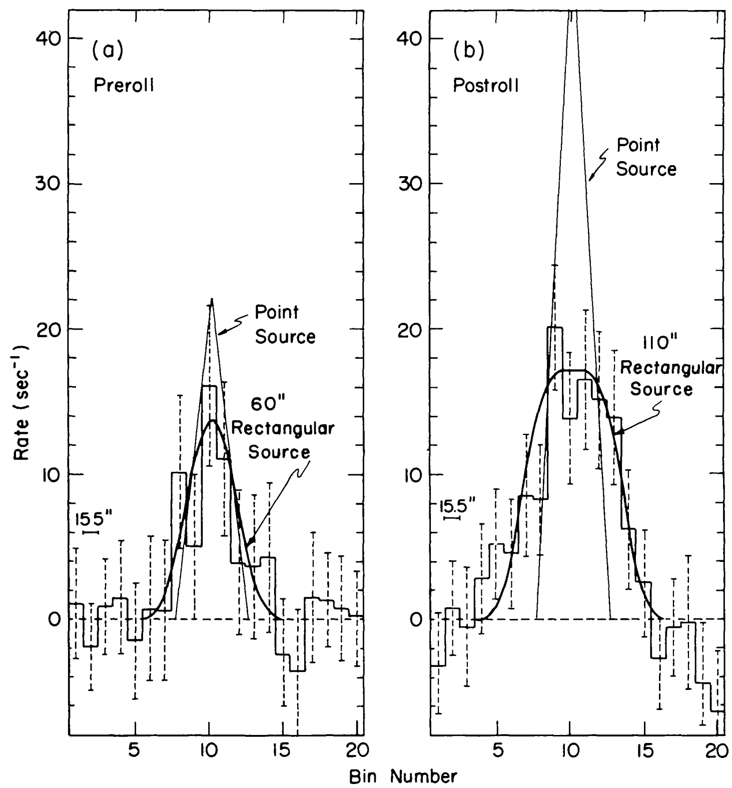

FIG. 2.—Summation of all data obtained during the preroll (postroll) hold on the Crab Nebula, plotted with background subtracted as a function of bin number. The error bars indicate one standard deviation and include the effect of the uncertainty in the background rates. The bin width (15.″46) is the mean of the long and short bin widths. The expected responses for point and rectangular source distributions are also presented.

In order to obtain celestial positions and angular sizes based on the entire data we superimposed the short and long data bin by bin for both the preroll and postroll observations (Fig. 2). Since the angular sizes of the long and short bins are different by 5 per cent, the straightforward bin-by-bin superposition smears the angular resolution, but at most by 7″ ($\frac{1}{2}$ bin) in bin 1 and bin 20. The effect on the rates is negligible. In Figure 2 we also show the expected responses with normalized areas of point sources and of rectangular sources of uniform intensity which best fit the data. In the case of the preroll data the most probable angular size is 60″ $\pm$ 60″ for the assumed rectangular shape. However, we cannot exclude a point source. During the postroll period the source spent a greater fraction of the time within the 40″ transmission zones. The data are therefore of better quality and yield an angular size of 110″ $\pm$ 25″. In this case a point source is clearly excluded. The quoted errors are based upon χ^2 tests of other source sizes and represent a probability of occurrence equal to that expected for 1 standard deviation in a normal distribution. As we will discuss later, these data are also consistent with an X-ray source region identical in shape and size to that of the optical source.

The total counting rates due to the source in the 1–6 keV region are 1.1 ± 0.3 cm^{-2} sec^{-1} and 2.1 ± 0.3 cm^{-2} sec^{-1} for the preroll and postroll data, respectively. These rates include the effects of the limited angular aperture (40″ FWHM) of the collimators and the reduction of effective counter area by the X-ray shadows of the collimator, grid, and counter-window support structures. The stated precision in these rates is statistical and arises, in part, from the statistical errors in the background measurements. The apparent

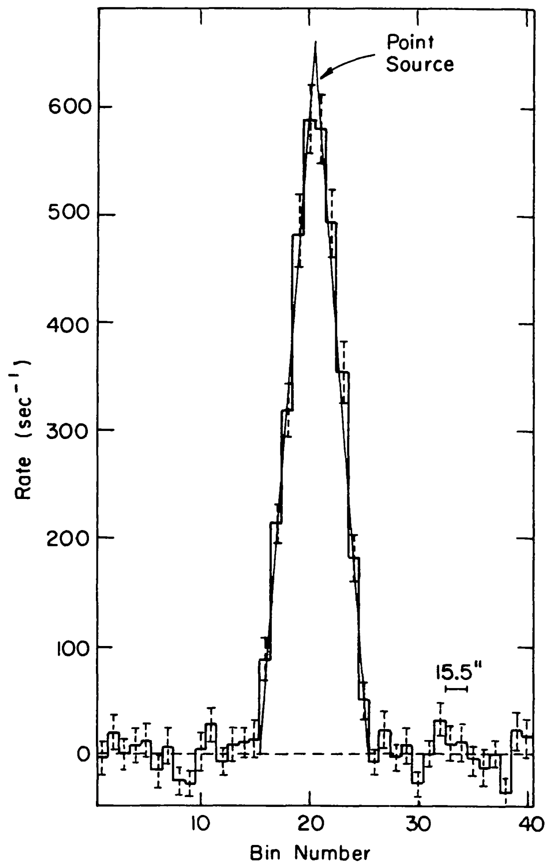

FIG. 3.—Superposition of all data obtained during "hold" portion ($289 < t < 302$ sec) of the Sco X-1 observations described by Gursky *et al.* (1966*a*, *b*).

discrepancy in the rates can be understood either as a statistical fluctuation in their difference of two standard deviations or as systematic errors in our initial assumptions as to which bins in Figure 1 represent true measurements of the background. We have found, however, that our conclusions regarding the size and location of the source are not significantly affected by the assumption of any other set of background levels which is compatible with the flight data.

To test this method of analysis we have carried out the same superposition techniques on the Sco X-1 data obtained later in the same flight (Fig. 3). The data indeed conform to a point source with a precision of about 15″, and, as previously reported, the line of position corresponding to the centroid of the peak lies within 20″ of the optical object Sco X-1.

The celestial position of the center of the Crab X-ray source is obtained from the intersection of the lines of position corresponding to the centroids of the peaks in Figure 2:

$$\alpha(1950.0) = 5^h31^m30^s ,$$

$$\delta(1950.0) = 21^\circ59'.1 .$$

The statistical errors (standard deviation) in the centroid determinations are 20″ and 15″ in the preroll and postroll data, respectively. The 15″ error in each of the many aspect determinations is random and produces negligible error in the centroid position.

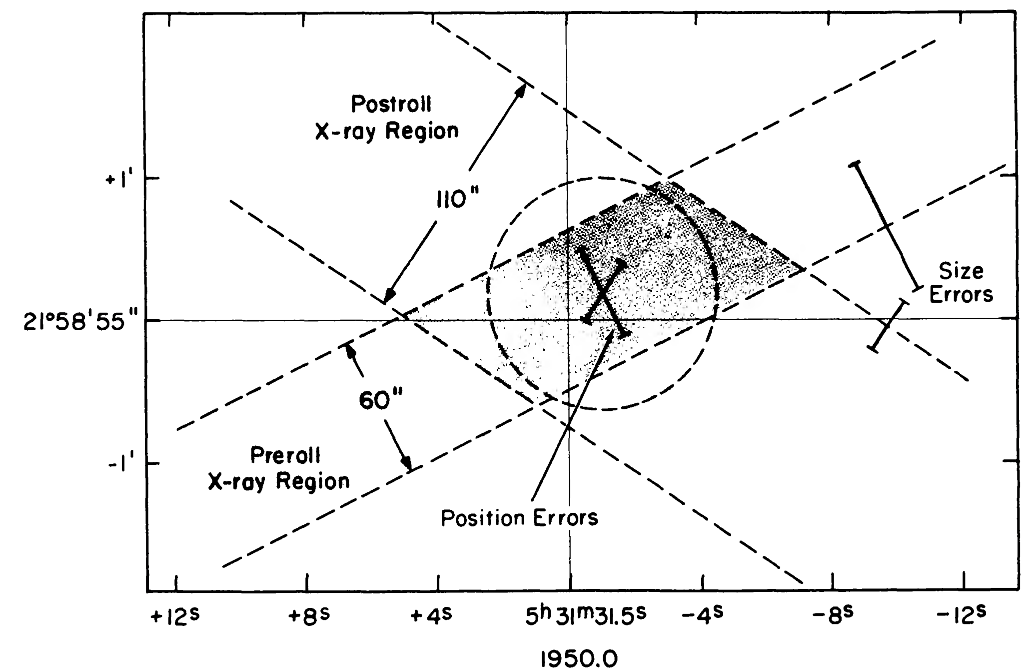

FIG. 4.—Celestial coordinates of the X-ray results presented in Fig. 2. The two lightly shadowed bands indicate the X-ray regions defined by the preroll and postroll scans, respectively, under the assumption of rectangular source distributions in each scan direction. The darkly shadowed area of intersection indicates the most probable X-ray source region under these assumptions. The error bars represent the statistical errors; the systematic errors in the position are estimated to be less than 15″. The size and shape of the source are idealized as a circular area of diameter 100″. The origin of the coordinate system is the southwest component of the central double star.

We previously estimated (Gursky *et al.* 1966*b*) that a systematic error of as much as 30″ could be introduced by uncertainties in the correlation of the optical fiducial pattern with the X-ray transmission directions and, probably more important, by errors in extrapolation across the film. We now believe that systematic errors for the Crab are somewhat smaller because (1) the discrepancy between the position of the optical object Sco X-1 and the position deduced from the flight data was, as mentioned above, only about 20″ and (2) the position of the Crab lay closer to the center of the field of view than did Sco X-1.

The position and size results from this experiment are presented schematically in Figure 4. The darkly shaded area represents the most probable X-ray source region. Because of the large statistical error in the preroll size result, we choose to report the circular area as an idealization of the size and shape of the X-ray source. Its diameter (100″) is obtained from a statistical weighting of the preroll and postroll data.

In Figure 5 (Plate L1) we have transferred these results to a Palomar photograph of

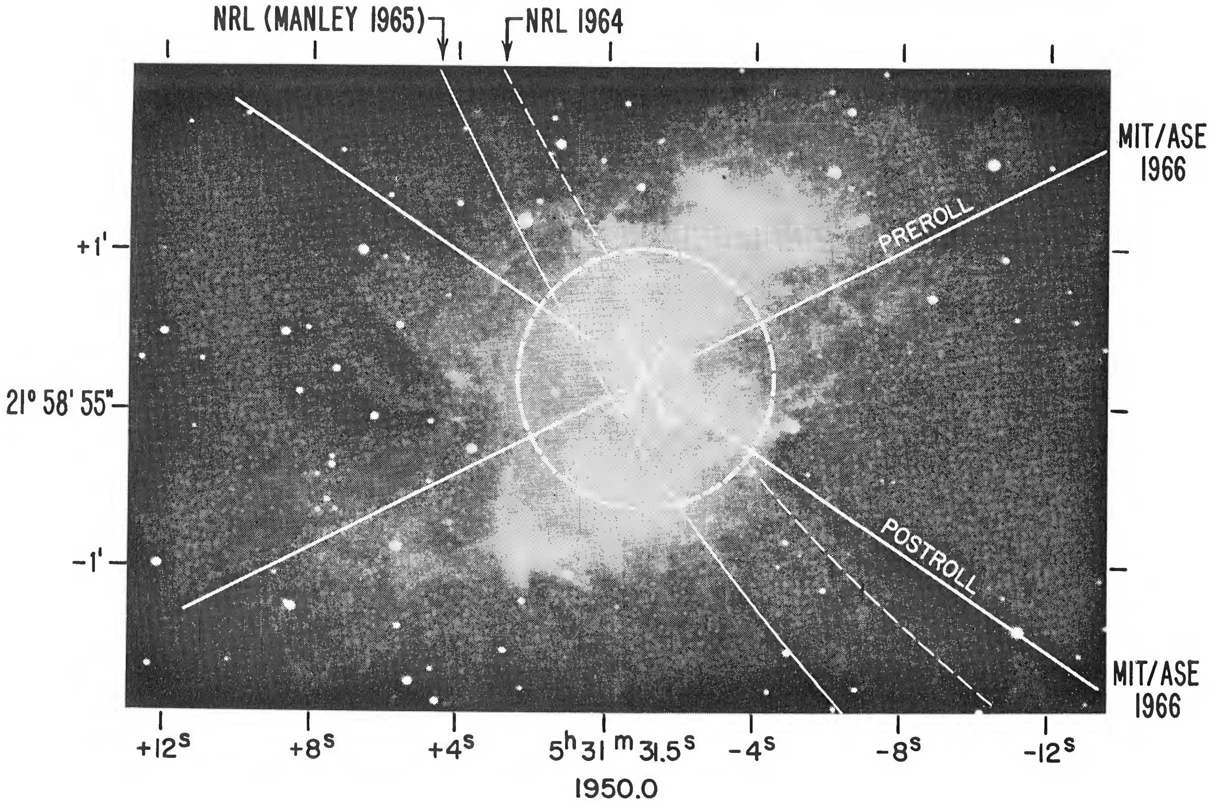

FIG. 5.—Summary of results pertaining to the position of the X-ray source in the Crab Nebula. The dashed curved line is the line of position obtained from a lunar occultation experiment by Bowyer *et al.* (1964), and the solid curved line is the same result corrected by Manley and Ouellette (1965) for parallax due to the motion of the rocket. The intersection of the two MIT/AS&E lines of position is at (1950.0) $\alpha = 5^h 31^m 30^s$, $\delta = 21° 59'.1$. The 100″ diameter circle, taken from Fig. 4, is an idealization of the source region. The origin of the coordinate system is the southwest component of the central double star.

ODA *et al.* (*see* page L9)

the Crab Nebula. The earlier results based on the occultation experiment are also shown. The dashed line, marked *NRL*, gives the originally reported (Bowyer *et al.* 1964) position of the lunar limb corresponding to the observed peak of the X-ray distribution. Manley and Ouellette (1965) have recently recalculated the lunar position taking into account parallax introduced by the rocket motion during the flight and their result is the solid line marked *NRL*. The effect of this parallax was to cause the limb of the Moon to almost double its rate of traversal across the Crab, and this, in turn, gives rise to an angular size of about 2′ rather than about 1′ as originally reported.

In order to make a more quantitative comparison between the distribution of visible light and X-rays, we integrated the light intensity in the directions normal to our X-ray scans using the contour map given by Woltjer (1957). The results are shown in Figure 6. It is seen that the centroids of the X-ray and visible light distributions agree well within the random error of the X-ray observations. We find that X-ray distribution functions of the same size and shape as the visible light distributions can easily be fit (with resulting χ^2 probabilities of 60 and 30 per cent) to the preroll and postroll data.

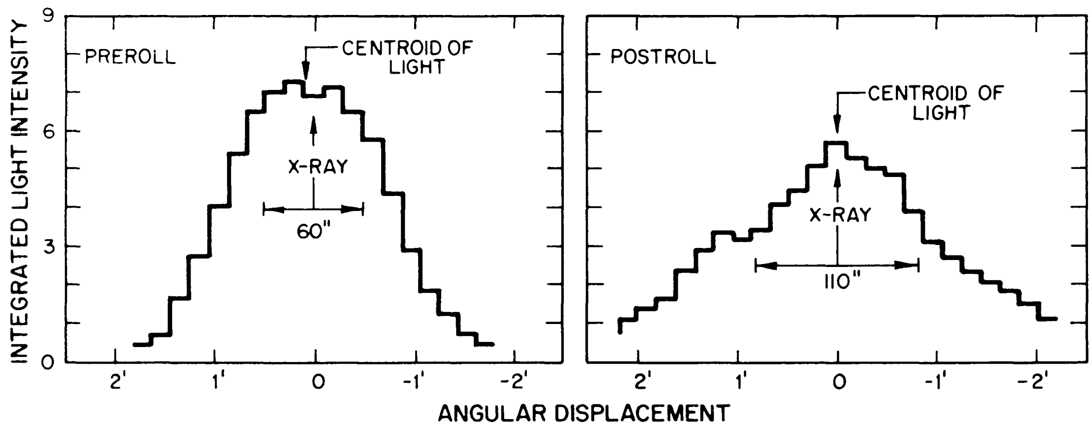

FIG. 6.—Visible light distributions as a function of angle along the preroll (postroll) scan direction as obtained from integrations, perpendicular to the scan direction, of the isophotes given by Woltjer (1957). The X-ray results are taken from Fig. 2.

In summary, this experiment yields two principal results. First, the X-ray and visible light distributions have a common center within the 15″ precision of the measurement. Second, the source has a finite angular extent. The data are consistent with X-ray emission regions which range in size and shape from uniform emission by the central two arc minutes of the Crab to a distribution identical to that of the visible light. These results place constraints upon the details of the possible models for X-ray emission. For instance, the markedly off-center features of the Crab, such as the maximum of the radio polarization at centimeter wavelengths (Gardner 1965; Allen and Barrett 1966) or the small diameter radio source at 25–40 mc/s (Andrew, Branson, and Wills 1964; Hewish and Okoye 1965), cannot be made to have a direct simple relation to the X-ray production.

We wish to thank the staffs of American Science and Engineering and of the Laboratory for Nuclear Science at Massachusetts Institute of Technology for their assistance throughout this experiment. We are grateful to Dr. Leo Sartori, Professor Philip Morrison, Professor L. Woltjer, and Dr. Oscar Manley for helpful discussions. We are further grateful for the support given us by the staffs of the Sounding Rocket Branch of Goddard Space Flight Center and the White Sands Missile Range. This work was supported in part through funds provided by the National Aeronautics and Space Administration under contracts NASw-1284 and NASw-1535 and grant NSG-386, and in part by the U.S. Atomic Energy Commission under contract AT(30-1)2098.

M. Oda*
H. Bradt
G. Garmire†
G. Spada‡
B. V. Sreekantan§

February 13, 1967
Massachusetts Institute of Technology
Cambridge, Massachusetts

H. Gursky
R. Giacconi
P. Gorenstein
J. R. Waters

American Science and Engineering, Inc.
Cambridge, Massachusetts

REFERENCES

Allen, R. J., and Barrett, A. H. 1966, presented at 123d meeting of the AAS, Los Angeles (abstract to be published in A.J.).
Andrew, B. H., Branson, N. J. B. A., and Wills, D. 1964, *Nature*, **203**, 171.
Bowyer, S., Byram, E. T., Chubb, T. A., and Friedman, H. 1964, *Science*, **146**, 912.
Gardner, F. F. 1965, *Australian J. Phys.*, **18**, 385.
Gursky, H., Giacconi, R., Gorenstein, P., Waters, J. R., Oda, M., Bradt, H., Garmire, G. and Sreekantan, B. V. 1966*a*, *Ap. J.*, **144**, 1249.
———. 1966*b*, *ibid.*, **146**, 310.
Hewish, A., and Okoye, S. E. 1965, *Nature*, **207**, 59.
Manley, O., and Ouellette, G. 1965 (private communication).
Morrison, P., and Sartori, L. 1967 (in press).
Sandage, A. R., Osmer, P., Giacconi, R., Gorenstein, P., Gursky, H., Waters, J. R., Bradt, H., Garmire, G., Sreekantan, B. V., Oda, M., Osawa, K., and Jugaku, J. 1966, *Ap. J.*, **146**, 316.
Shklovskii, I. S. 1966, *Astr. Zh.*, **43**, 10 (English trans. in *Soviet Astr.—AJ*, **10**, 6, 1966).
Woltjer, L. 1957, *B.A.N.*, **13**, 302.
———. 1964, *Ap. J.*, **140**, 1309.

* Presently at Institute of Space and Aeronautical Science, University of Tokyo, Tokyo, Japan.
† Presently on leave at California Institute of Technology, Pasadena, California.
‡ On leave from the Laboratorio di Astrofisica, Frascati, Italy.
§ Presently at the Tata Institute of Fundamental Research, Bombay, India.